https://doi.org/10.2352/issn.2168-3204.2023.20.1.27


# Do-It-Yourself LUT-based Linearization of Image Sensors

***Maximilian Czech, Giorgio Trumpy, Ali Raza Syed; Norwegian University of Science and Technology; Gjøvik, Norway***

## Abstract

*Imaging sensors are linear over a large part of their operational range. Nevertheless, their behavior becomes non-linear when approaching saturation. This is undesired if such sensors are used for scientific measurements. In this work, a simple and efficient off-chip method is proposed for image sensor linearization. First, the sensor response is characterized with a constant irradiance and a sequence of captures at several integration times. Then a 1D look-up table is calculated to compensate for the nonlinear range. This LUT can be applied to the raw sensor data before further postprocessing. The higher signal-to-noise ratio of captured data is used to demonstrate the benefit of the extended linear range. The proposed method can restore linearity while being easy to implement and computationally efficient.*

## Introduction and related work

Although the linearity of current image sensors (CCD and CMOS) in respect to incoming radiance spans over a large region of their operational range, their behavior becomes nonlinear when approaching the saturation point. This can be caused by many factors, such as an applied gain, the nonlinear integration capacitor of the source follower or the analog-to-digital converter [1]. On the other hand, to capture an image that uses the widest possible range of the sensor's dynamics, it is desired to set the camera parameters in a way that a maximum amount of light is captured without reaching the saturation point, so the signal-to-noise ratio (SNR) is optimized. This procedure is often referred to as "exposing to the right" (ETTR) [2], since the values of the resulting histogram would be shifted to the right side. In some applications, for example artistic or documentary photography, the resulting nonlinear relation between incoming photons and the detected sensor response is not problematic or is even desired since a compression of highlights can be oftentimes beneficial. However, when such an imaging sensor is used for scientific measurement of light, the nonlinear behavior will cause significant errors in the resulting data. Therefore, the capturing of linear data is of great importance. There is no general recommendation, but a non-written agreement within the scientific community suggests using 2/3 or 3/4 of the dynamic range, so that the nonlinear region of the sensor is avoided. As a drawback, a limited portion of the sensor's dynamic range is used, which leads to a reduced SNR.

The proposed method of linearization using a LUT applied to the raw data allows for ETTR and therefore using more of the available dynamic range of a given imaging sensor, while maintaining the linear relation between the incoming radiance and the unprocessed sensor data. Other approaches were taken in the past to improve the linearity of imaging sensors. Often, existing methods for linearization of sensor responses aim at hardware and circuit optimizations [3]. A broad variety of approaches were taken, such as piece-wise linearizing circuits for highly nonlinear sensors [4], combined multigated transistors and capacitance compensation for the linearization of CMOS Broadband Power Amplifiers [5]. But also, on the software side many improvements were proposed using LUT-based approaches. In 2012 Bengtsson evaluated the optimum of look-up table sizes in small embedded systems with limited memory and computational power [6]. The authors state that a LUT that is used in such a system should be big enough to minimize the introduced errors of the interpolation, but preferably small in size to reduce computation time during the application for real time processing on systems with limited computational power. Balestrieri et al. reviewed the use of LUTs and other methods to compensate for error sources within A/D-converters [7]. The performance of low precision analog to digital converters were improved by Frey and Loeliger using a look-up table approach [8]. Efforts were made by Dinstein et al. to perform a LUT linearization for imaging systems [9]. The authors carried out a subtraction for dark current noise and then applied a LUT that was obtained by fitting the measured system response to an analytical curve. A review on different approaches implemented using a field programmable gate array was published by Sonawal et al. [10]. Unlike other existing work, the present paper proposes a method with a straightforward implementation that compensates for the nonlinear behavior of an imaging sensor after capturing the data. The correction is not implemented on-chip but is instead applied to the captured image data after the offload from the camera as a first step in the postprocessing pipeline. The necessary measurements are easy to obtain and do not require specialized equipment. This makes the method applicable for a large variety of use cases with different imaging systems where improved sensor linearity is of importance.

## Methodology

In this work, the possibility of using an easy to implement 1D look-up table (LUT) is proposed to enhance the linearity of a monochromatic CMOS sensor after data acquisition. A look-up table approach has certain advantages such as a straightforward and computationally efficient implementation. First, the camera sensor is characterized in terms of its linearity. Then, the creation of the LUT for compensating the nonlinear region of the sensor is described in detail. Afterwards, the evaluation process is presented and discussed.

### *Sensor characterization*

The camera used was a monochromatic QHY600 designed for scientific measurements and sky survey manufactured by QHYCCD [11]. Built in is a native 16bit back-illuminated full frame CMOS sensor type IMX455 manufactured by Sony. The spatial resolution is 9576×6388 pixel, with a pixel size of 3.76×3.76 µm. The camera delivers unprocessed data from the sensor without any postprocessing such as hot pixel removal or noise reduction [11]. The QHY600 was used in an existing setup build by Trumpy et al. [12] for capturing multispectral transmittance data of analog film slides. In the presented experiments, one band of this multispectral imaging device was used to measure the sensor response as well as to capture the test data to evaluate the performance of the calculated LUT via signal-to-noise ratio (SNR). The camera sensor was illuminated using one narrow-band LED at maximum intensity with peak wavelength at 625nm and a full-width-half-maximum of around 15nm. By using the exposure times offered in the camera software, it was possible to cover the full dynamic range of the sensor. An adjustment of the power output of the LED through pulse-width-modulation was not considered since this would introduce phase problems, which result in a stripe-wise noise in the images due to the rolling shutter of the specific camera used. In order to avoid the heating of the LED and a consequent change of its emission, a heat dissipation system was used, and the LED was kept on just during the camera's integration time. In general, any light source with good emission stability is suitable for this method.

The sensor response was controlled by varying the image exposure. Thirty equally spaced integration times were chosen between 0.1ms and 35ms to capture monochromatic images over the full sensor range for its characterization. It must be noted that even at complete saturation, the sensor response did not reach the highest limit of the dynamic range, which would result in a digital number (DN) of 65535. The highest measured response in this experiment was around 63400 DN, and a further increase in the exposure time would not result in a higher response. This might be due to an internal limiter in the camera software and should be further investigated.

The measured sensor response (blue line) and the ideal response of the corresponding sensor with a linear behavior across the whole dynamic range (dotted red) are plotted in *Figure 1*. The ideal response was obtained in three steps. First, the slope between each pair of subsequent measured datapoints, indicated as blue dots in *Figure 2*, obtained with different exposure times was calculated and the significant changes in the distribution of the calculated slopes were identified using the method described by Killick et. al. [13]. In our case, these change points describe the start and the end of the linear sensor region. The red circle in *Figure 1* indicates the point, where the real sensor response starts to deviate from linearity, at about 42000 DN.

To avoid the influence of noise in regions of low sensor response on the calculation of the linear region, the measurements with extremely low exposure time were excluded from the calculation and the change point was set to 8200DN. By carrying out a linear extrapolation of the line that is described by the two change points, the ideal linear sensor response was obtained over the whole 16bit range of the sensor.

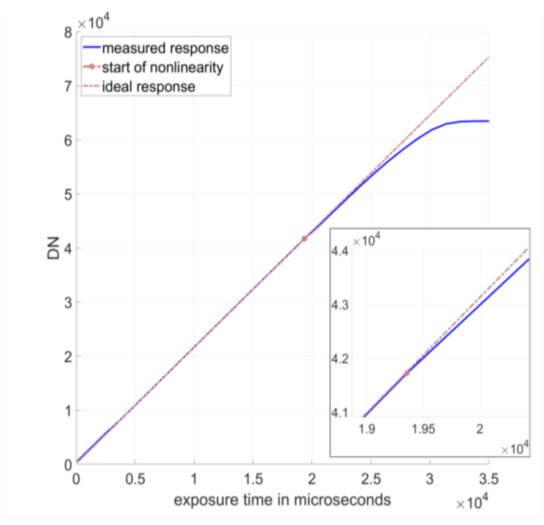


*Figure 1. Deviation of the real response from an ideal linear response*

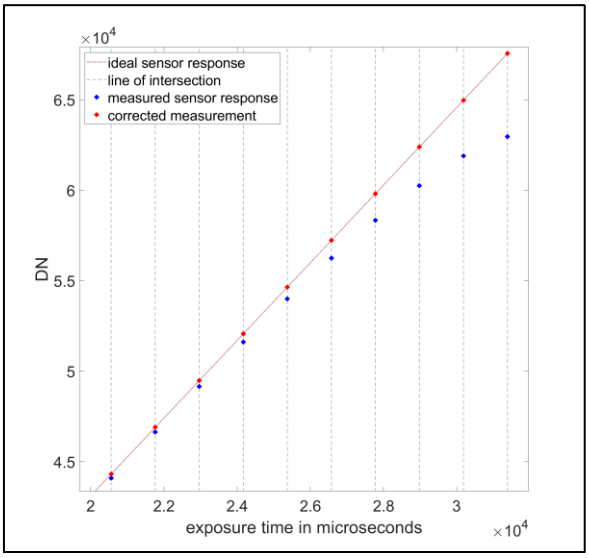


*Figure 2. Calculated intersection points between measured response and ideal response.*

## Creating the look-up table

We propose a method to create a 1D lookup table (1D-LUT) that adjusts for the non-linearity of the CMOS sensor. The method consists of the following steps.

First, the nonlinear region of the sensor is identified, and the ideal response curve is obtained as described in the previous section. Then, for each measurement in the nonlinear range, the corresponding value on the ideal response curve is determined. This is done by identifying the DN of the ideal response curve at the exposure value of the corresponding measurement, as shown in *Figure 2.* Since we know the equation of the line for the ideal response curve, we can determine its DN for every possible value of exposure times.

The result is a linearized response curve consisting of a total of the 30 corrected measurement points. Next, linear interpolation is used to find the DNs between the measured exposure times. This way, the DN corresponding to the ideal linear response can be determined for any DN corresponding to a real image capture. The digital numbers above 65535 are clipped and the final look-up table is exported as .txt file.

## Evaluation process

A step wedge with three bars of neutral density filter was selected for the evaluation as shown in *Figure 3*. The optical densities of the three bars are 1.76, 2.62 and 3.38.

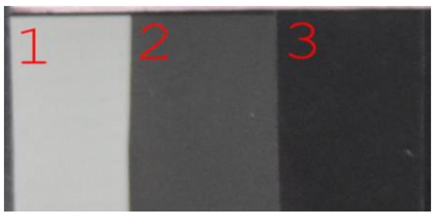


*Figure 3. Image of the step wedge that was captured to analyze the performance of the LUT. The number of layers of the ND filter are indicated.*

Three images of the step wedge were taken with the imaging system. The exposure time of the camera was set so that the resulting output using no sample between the light source and the sensor was limited to a maximum digital number, aiming for 58000 DN ($I_{58}$), 40000 DN ($I_{40}$), and 20000 DN ($I_{20}$). While $I_{40}$

roughly corresponds to the end of the linear region of the sensor, $I_{58}$ aims for much higher maximum digital numbers to test the LUT. $I_{20}$ was chosen as an extreme case where a low signal to noise ratio can be expected. An overview is given in *Table 1*.

**Table 1: overview over the aimed $DN_{MAX}$ of the captures.**

| Capture | aimed $DN_{MAX}$ | Note |
|---|---|---|
| $I_{58}$ | 58000 DN | To apply the LUT created for linearization |
| $I_{40}$ | 40000 DN | Roughly the limit of the native linear sensor response |
| $I_{20}$ | 20000 DN | Extreme case, small SNR expected |

All images were captured slightly 'out of focus', to avoid the potential influence of small dust particles and micro-scratches on the evaluation results. For each aimed $DN_{MAX}$, the white and black frame were recorded. Then, a flat-fielding process was carried out to obtain transmittance values. For the flat-fielding, Eq. (1) was used, where $I_{RAW}$ is the capture of the step wedge, $I_W$ is the corresponding white frame without sample, $I_B$ is the black frame, and $I_{FF}$ is the resulting flat-fielded image. For $I_{58}$, the LUT was applied to $I_{RAW}$ as well as to the corresponding white frame to linearize the sensor response before the flat-fielding process.

$$I_{FF} = \frac{I_{RAW} - I_B}{I_W - I_B} \quad (1)$$

From each image, a portion with a spatial resolution of 500x1500 pixels was cropped out from the center of each of the steps indicated in *Figure 3*. For each step, the cropped portions will be referred to as $aim_{58+LUT}$ (cropped wedge from $I_{58}$ including the LUT), $aim_{58}$ (cropped wedge from $I_{58}$ without LUT), $aim_{40}$ (cropped wedge from $I_{40}$) and $aim_{20}$ (cropped wedge from $I_{20}$). The cropped sections were then evaluated by comparing the mean (μ), standard deviation (σ), and the signal-to-noise ratio (SNR). The signal-to-noise ratio can be calculated by using Eq. (2).

$$SNR = \frac{\mu}{\sigma} \quad (2)$$

To verify that the method can be used for a broad range of imaging sensors, additional camera models were characterized and a look-up table for linearization was created for each of the cameras, following the same approach as explained in the previous sections. The additional cameras were a Canon G7 and a Silios CMS-S multispectral camera. The resulting measured and corrected response curves are shown below.

In addition, to evaluate the method in a real-world scenario, the Canon G7 was used to capture a 35mm analog film slide displaying a Kodak LAD-girl amongst some reference patches at different aim values (60.000DN and 40.000DN in 16bit range). Again, the LUT was applied to the capture that was exposed 'to the right'. The visibility of noise in the captured images was then visually evaluated.

## Results

The camera response curve after the linearization process of the different camera models QHY600, Canon G7 and Silios CMS-S are shown in *Figure 4, Figure 5* and *Figure 6* respectively. The proposed method extends the linear response region of the sensor significantly. The results from analyzing the noise present in the different steps of the wedge for the different images aimed at different maximum DN are shown in *Table 2, Table* 3 and *Table 4*.

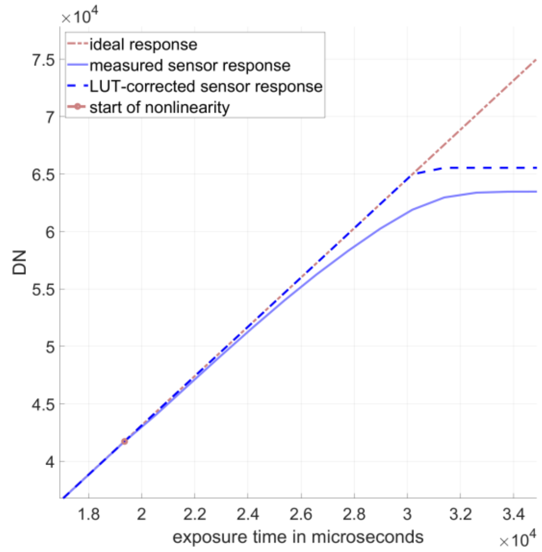


*Figure 4. Closeup of the measured and LUT-corrected response curves for the QHY600.*

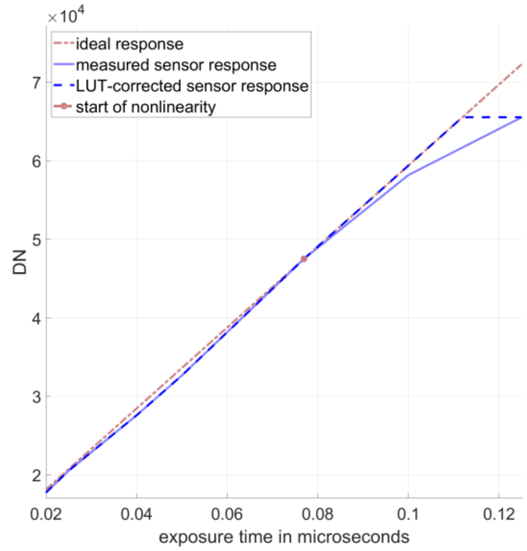


*Figure 5. Closeup of the measured and LUT-corrected response curves for the Canon G7.*

For a perfect linear sensor, the mean values of each step are assumed to be consistent after carrying out the flat fielding operation, while the standard deviation gives information about the intensity of the noise within each image. Since $aim_{40}$ uses the full liner range of the sensor while avoiding the nonlinear region, its values are used as reference. As can be seen in *Table 2*, an exposure aiming for 58.000DN at maximum produces wrong mean values, while the image with applied LUT restores the mean towards the reference to a large extend, giving accurate linear values. At the same time, the standard deviation is improved when using $aim_{58+LUT}$. Therefore, the SNR greatly improves when comparing $aim_{58+LUT}$ with $aim_{40}$, reducing the influence of the noise. As expected, the SNR increases with the aimed max-value but is not affected by the look-up table.

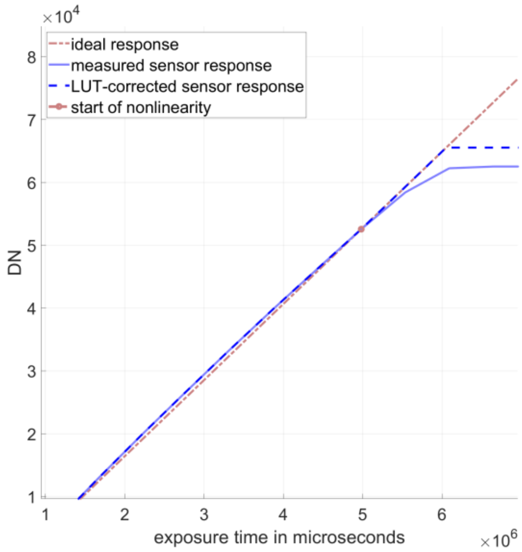


*Figure 6. Closeup of the measured and LUT-corrected response curves of the Silios CMS-S.*

**Table 2: noise analysis results for step nr. 1.**

| sample | mean (µ), DN | std.dev. (σ), DN | SNR |
|---|---|---|---|
| $aim_{58+LUT}$ | 993.231 | 34.189 | 29.051 |
| $aim_{58}$ | 1004.615 | 34.398 | 29.205 |
| $aim_{40}$ | 995.926 | 42.828 | 23.254 |
| $aim_{20}$ | 994.649 | 62.245 | 15.979 |

**Table 3: noise analysis results for step nr. 2.**

| sample | mean (µ), DN | std.dev. (σ), DN | SNR |
|---|---|---|---|
| $aim_{58+LUT}$ | 122.105 | 14.022 | 8.708 |
| $aim_{58}$ | 123.58 | 14.157 | 8.729 |
| $aim_{40}$ | 120.451 | 18.64 | 6.462 |
| $aim_{20}$ | 112.741 | 32.653 | 3.453 |

**Table 4: noise analysis results for step nr. 3.**

| sample | mean (µ), DN | std.dev. (σ), DN | SNR |
|---|---|---|---|
| $aim_{58+LUT}$ | 12.74 | 8.451 | 1.508 |
| $aim_{58}$ | 12.91 | 8.533 | 1.513 |
| $aim_{40}$ | 12.905 | 10.903 | 1.184 |
| $aim_{20}$ | 12.654 | 16.898 | 0.749 |

When visually comparing the green channel of the captured 35mm slide with the look-up table applied (aiming at 60.000DN) against the ones exposed to a maximum DN of 40.000 and 20.000 a decreased amount of noise is observable. *Figure 7* shows a cropped portion of the captured slide at different aim values. The results are promising and indicate that the proposed method works successfully and can be applied in real world scenarios.

## Conclusions and future work

The evaluation of the proposed method indicates that the non-linearity of a given imaging sensor can be corrected by characterizing the sensor response throughout its whole range and compensate for the nonlinear regions by applying a look-up

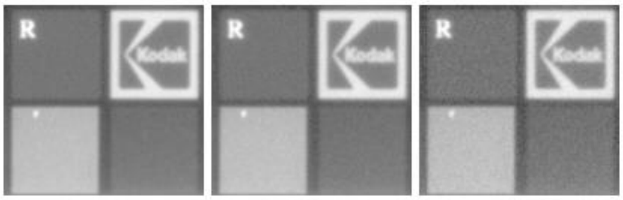

*Figure 7. Comparison of the noise present in the captured 35mm slide. Left: aim60+LUT, middle: aim40, right: aim20.*

table. The implementation does not add a significant complexity to the postprocessing pipeline of the raw data obtained by the sensor and gives reasonable results. The evaluation results show that using the proposed LUT-based approach allows to expose samples and scenes further 'to the right', thus increasing the signal-to-noise ratio of the captured data. As a result, higher digital numbers can be obtained, and a greater region of the given sensor is effectively used without sacrificing a linear correlation between incoming photons and the sensor response. This leads to a reduction of the impact of among others dark current and static sensor noise. The proposed method is applicable and easy to compute for single and multichannel systems, as well as for different sensor types. It must be noted that temperature changes of the imaging system were not considered during this project, which might require further evaluation.

## References


[1] F. Wang and A. Theuwissen, "Linearity analysis of a CMOS image sensor," *Electronic Imaging,* vol. 29, p. 84–90, January 2017.

[2] "Expose (to the) Right," Luminous Landscape, 2003. [Online]. Available: https://web.archive.org/web/20150209012804/http://www.luminous-landscape.com/tutorials/expose-right.shtml. [Accessed 02 03 2023].

[3] H. Zhang and E. Sanchez-Sinencio, "Linearization Techniques for CMOS Low Noise Amplifiers: A Tutorial," *IEEE Transactions on Circuits and Systems I: Regular Papers,* vol. 58, p. 22–36, January 2011.

[4] D. N. Mahaseth, L.Kumar and T. Islam, "An efficient signal conditioning circuit to piecewise linearizing the response characteristic of highly nonlinear sensors," *Sensors and Actuators A: Physical,* vol. 280, p. 559–572, September 2018.

[5] C. Lu, A.-V. H. Pham, M. Shaw and C. Saint, "Linearization of CMOS Broadband Power Amplifiers Through Combined Multigated Transistors and Capacitance Compensation," *IEEE Transactions on Microwave Theory and Techniques,* vol. 55, p. 2320–2328, November 2007.

[6] L. E. Bengtsson, "Lookup Table Optimization for Sensor Linearization in Small Embedded Systems," *Journal of Sensor Technology,* vol. 02, p. 177–184, 2012.

[7] E. Balestrieri, P. Daponte and S. Rapuano, "A State of the Art on ADC Error Compensation Methods," *IEEE Transactions on Instrumentation and Measurement,* vol. 54, p. 1388–1394, August 2005.

[8] M. Frey and H.-A. Loeliger, "On flash A/D-converters with low-precision comparators," in *IEEE International Symposium on Circuits and Systems*, 2006.

[9] I. Dinstein, F. Merkle, T. D. Lam and K. Y. Wong, "Imaging System Response Linearization And Shading Correction," *Optical Engineering,* vol. 23, December 1984.

[10] D. Sonawal and M. Bhuyan, "Multi channel sensor linearization in field programmable gate array for real time applications," *Sensors & Transducers,* vol. 191, p. 135, 2015.

[11] *QHYCCD Scientific Camera QHY600PRO,* https://www.qhyccd.com/scientific-camera-qhy600pro-imx455, last accessed: 2022-11-30.

[12] G. Trumpy, J. Y. Hardeberg, S. George and B. Flueckiger, "A multispectral design for a new generation of film scanners," in *Optics for Arts, Architecture, and Archaeology VIII*, 2021.

[13] R. Killick, P. Fearnhead and I. A. Eckley, "Optimal Detection of Changepoints With a Linear Computational Cost," *Journal of the American Statistical Association,* vol. 107, p. 1590–1598, October 2012.

## Author Biography

**Maximilian Czech** obtained his Bachelor of Engineering in Audiovisual Media at Stuttgart Media University with focus on movie-postproduction. Currently he is an Erasmus+ Joint master's student (M.Sc.) in Computational Color and Spectral Imaging (COSI) at NTNU, Norway and Universidad de Granada, Spain. His main interests are the processing of color and hyperspectral image data as well as spectral image acquisition techniques.

**Giorgio Trumpy** is Associate Professor at the Norwegian University of Science and Technology and member of the Colourlab in Gjøvik. His main interests are optics and spectroscopy, colorimetry and image processing, heritage conservation and visual arts.

**Ali Raza Syed** is a master's student studying computational color and spectral imaging (COSI) at NTNU (Norway), UGR (Spain), and UEF (Finland). He is currently working on his master's thesis in collaboration of COSI and Munsell Color Science Laboratory at RIT (USA) related to embedding high dynamic range techniques in multispectral imaging in the context of cultural heritage. He has an academic background in computer engineering and industrial experience as a software engineer. His current interests lie in computer vision, color science, and hyperspectral imaging.